

CoA: Chain-of-Action for Generative Semantic Labels

Meng Wei¹, Zhongnian Li¹, Peng Ying¹, Xinzheng Xu¹

¹School of Computer Science and Technology, China University of Mining and Technology, Xuzhou, China

mengw@cumt.edu.cn, zhongnianli@cumt.edu.cn, pengying@cumt.edu.cn, xxzheng@cumt.edu.cn

Abstract

Recent advances in vision-language models (VLM) have demonstrated remarkable capability in image classification. These VLMs leverage a predefined set of categories to construct text prompts for zero-shot reasoning. However, in more open-ended domains like autonomous driving, using a predefined set of labels becomes impractical, as the semantic label space is unknown and constantly evolving. Additionally, fixed embedding text prompts often tend to predict a single label (while in reality, multiple labels commonly exist per image). In this paper, we introduce CoA, an innovative Chain-of-Action (CoA) method that generates labels aligned with all contextually relevant features of an image. CoA is designed based on the observation that enriched and valuable contextual information improves generative performance during inference. Traditional vision-language models tend to output singular and redundant responses. Therefore, we employ a tailored CoA to alleviate this problem. We first break down the generative labeling task into detailed actions and construct an CoA leading to the final generative objective. Each action extracts and merges key information from the previous action and passes the enriched information as context to the next action, ultimately improving the VLM in generating comprehensive and accurate semantic labels. We assess the effectiveness of CoA through comprehensive evaluations on widely-used benchmark datasets and the results demonstrate significant improvements across key performance metrics. Our source code is available at: <https://github.com/WilsonMqz/CoA>

1. Introduction

Visual-language models have achieved significant success in various downstream tasks encompassing both vision and language, particularly in image classification tasks [3, 16, 18, 36]. These models demonstrate remarkable results in zero-shot image classification tasks by aligning the semantics of vision and language [23, 24, 29, 34]. However, this alignment relies on a predefined set of categories (as illustrated on the left of Fig. 1), achieved by constructing em-

bedding templates such as “a photo of a class” for zero-shot reasoning [23, 34]. This assumption becomes impractical with the increasingly vast real-world data scale where semantic label spaces are often unknown and continuously evolving [8, 27, 50]. For instance, in domains like autonomous driving and robot vision, data collected in complex environments is diverse, while label spaces dynamically evolve over time [13, 14, 25, 42].

In this work, we consider removing the assumption of a predefined set of labels and focus on directly assigning semantic-level labels to an image in a more unbounded environment, known as Generative Semantic Labels (GSLs). It is worth noting that the problem we address differs significantly from the traditional open vocabulary problem, which assumes the model has knowledge of and access to the list of target classes during inference [23, 24, 34]. Coinciding with our approach, Conti et al. [8] introduced Vocabulary-free Image Classification (VIC), which aims to assign a single label to an image without the assumption of predefined set of categories. However, they need to search through a vast visual-language library to find a similar semantic sentence for the image, essentially providing a larger semantic space. On the other hand, VIC’s objective is to match every image with one label, which is unrealistic in practical downstream tasks like semantic segmentation and object detection, where each image often has multiple labels (as depicted on the center of Fig. 1). Therefore, this inspired us to investigate a novel approach capable of predicting all labels within an image without assumption for a predefined semantic space.

In recent years, Large Multimodal Models (LMMs) such as LLaVA [29], GPT-4V [1], and InstructBLIP [9] have showcased impressive advancements in the realm of vision and language (VL), particularly in multimodal reasoning and visual question-answering (VQA). Therefore, we naturally consider two straightforward approaches to handle the GSLs task: VQA-based LMMs, which directly ask questions to obtain entity labels, and Caption-based LMMs, which first generate captions and then filter relevant entity labels. However, as shown in Fig. 2, VQA-based methods produce semantically overlapping labels, while Caption-

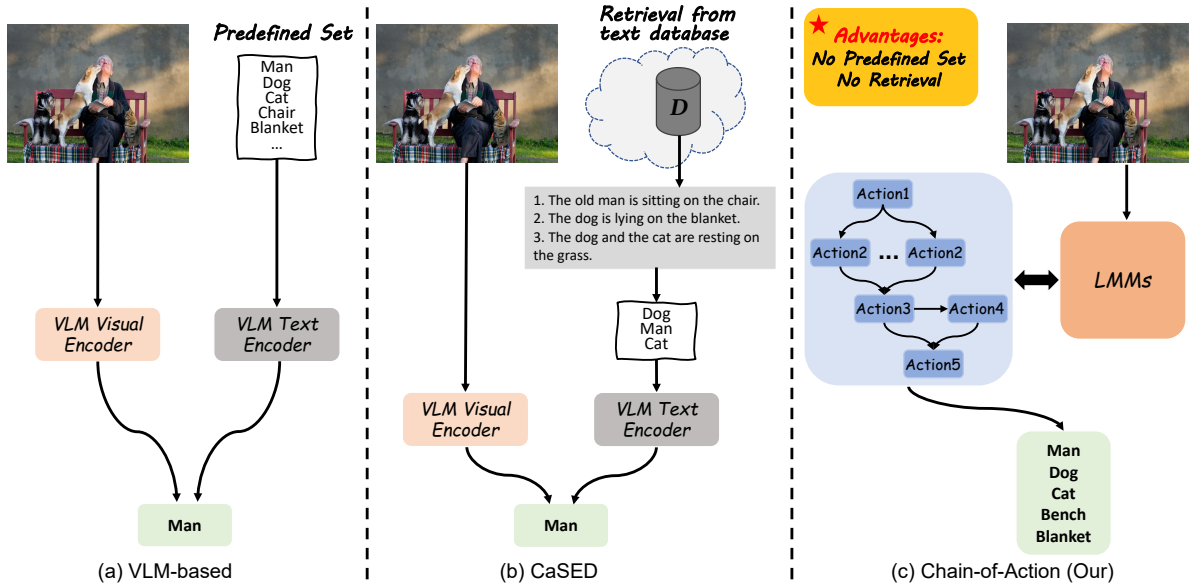


Figure 1. Comparison of the proposed method with other methods. (a) Vision-Language Model (VLM)-based methods operate under the assumption of a predefined set of target categories and typically output a single label per image. (b) CaSED removes the constraint of predefined categories but requires retrieval from an extensive text database and still ultimately predicts only a single label. (c) In contrast, our proposed Chain-of-Action (CoA) method simultaneously predicts multiple labels for an image without the need for predefined categories or retrieval, offering a more comprehensive and direct approach to semantic-level classification.

based methods tend to generate background or extended semantic labels—both of which are not well-suited for GSLs. Further discussion and analysis are provided in Section 3.2.

In this paper, we introduce a zero-shot, free vocabulary Chain-of-Action (CoA) method to better handle GSLs task. Our approach is designed on the observation that enriching the inference process with valuable contextual information leads to enhanced model performance [31, 46]. This capability of context-based prompting has also been widely validated in the application of large language models [21, 44]. In our work, we define a single interaction with LMMs as an individual action and design a progressive hierarchical chain-of-action structure to guide LMMs in generating the semantic labels. Initially, we leverage LMMs to produce an overall description of the test image, extracting and consolidating key local information. We then refine the representation of the key entities and their interrelationships, using this structured data as context. This progressive structure enriches the contextual understanding of LMMs, ultimately facilitating more comprehensive and precise label prediction. Our approach aligns with the principles of In-Context Learning by enhancing generative performance through contextual utilization but diverges by eliminating the need for similar, unrelated examples or additional data. Instead, it utilizes the inherent capabilities of LMMs and is adaptable across various models.

To quantitatively assess the performance of methods addressing GSLs task, we introduced a set of metrics to measure how effectively the predicted semantic labels align with

	Boat	Train	Screen
VQA-based	Boat Smaller boats	Train	Screen TV Person
Caption-based	Boat Night Dock	Train People	Screen Person Remote control
Human-labeled	Boat	Person Train	Tvmonitor
CoA	Large cargo ship Crane Dock	Train People Train station	Computer monitor Keyboard Mouse Wooden desk

Figure 2. Comparison of various settings, including VQA-based, Caption-based, Human-labeled and the proposed CoA method. VQA-based approaches often suffer from significant semantic redundancy, while Caption-based methods tend to identify background-related or extended semantics. In our evaluation, the dataset-provided labels are used as human annotations, which are relatively limited. Areas that are ignored are highlighted and the proposed CoA method generates results that are more comprehensive, diverse, and accurate.

the test image. Across all tasks and metrics, our methods consistently outperform all baselines, including sophisticated VLMs such as BLIP-2 and Instruct-BLIP. It is worth mentioning that our approach is simple yet effective and can serve as a competitive baseline for future research endeavors aimed at addressing the challenging GSLs task.

In summary, our main contributions are as follows:

(1) We explore a new task of generating semantic-level labels in a more open environment, eliminating the assumption of predefined label sets in VLMs. We formalize this task and propose specific evaluation metrics that can serve as a guideline for future studies.

(2) We introduce a customized zero-shot Chain-of-Action (CoA) approach that effectively guides LMMs in producing comprehensive and accurate semantic labels. Additionally, our CoA method is adaptable across various LMMs architectures.

(3) Our approach demonstrates enhanced performance across various benchmark datasets and all metrics.

2. Related Work

2.1. Large MultiModal Models (LMMs)

Recent advancements in Large Multimodal Models (LMMs) [2, 9, 10, 24, 28, 29, 43, 57] have successfully integrated the sophisticated reasoning abilities [35, 38] of large language models with visual-language models (VLM) [16, 23, 34], leading to significant breakthroughs in a wide range of downstream tasks. These tasks include, but are not limited to, Visual Question Answering (VQA) [3, 17–19, 30, 36], image-to-text generation, and text-to-image synthesis. Current approaches in LLMs predominantly focus on two core strategies: the alignment of image-text features and instruction fine-tuning.

Image-Text Feature Alignment. The image-text feature alignment approach is exemplified by CLIP [34], a pioneering work in the multimodal domain. CLIP employs 400 million image-text pairs to align text and image features within a shared embedding space. Building on this foundation, BLIP [23] integrates visual-text comprehension and generation within a unified multimodal framework, utilizing joint pre-training on three key objectives: image-text contrastive learning, image-text matching, and image-conditioned language modeling. Further advancing this line of work, BLIP-2 [24] capitalizes on pre-trained VLM to enhance multimodal performance and streamline the training process.

Instruction Fine-Tuning. In the instruction fine-tuning paradigm, InstructBLIP [9] integrates instruction-based inputs to guide both the Q-former and the large language model (LLM). Mini-GPT4 [58] employs a projection layer to bridge a visual encoder with a more advanced LLM, focusing training exclusively on this projection layer. Similarly, LLaVA [29] leverages GPT-4 [1] to generate multimodal instruction-following vision-text data and connects the visual encoder to the LLM via a projection layer, which is trained using an autoregressive model loss.

These approaches predominantly explore contrastive learning techniques to investigate refine graph-text feature alignment and enhance instruction fine-tuning capabilities. Although they have achieved significant success in complex

tasks related to image-text comprehension and generation, these methods exhibit limitations in handling simpler classification tasks. One-step generative answers are often redundant, primarily due to the rich semantics embedded in the image-text training data of LLMs. In contrast, our approach utilizes a step-by-step process to guide LLMs in generating more comprehensive and accurate information.

2.2. Large language models / Chain-of-Thought

Large language models (LLMs) [6, 11, 33, 35, 38, 39, 49, 51] have garnered significant attention in recent years due to their ability to understand and generate natural language text. Models like GPT-3 [6] and LLaMA [39] have demonstrated impressive performance across various natural language processing tasks. These models are typically pre-trained on massive text data and fine-tuned on specific downstream tasks [11, 39, 49]. They have been employed in applications such as text generation, translation, summarization, and question answering. Research efforts have focused on enhancing the capabilities, efficiency, and interpretability of these large language models.

The chain-of-thought (CoT) [5, 22, 40, 41, 45, 47, 48, 53–56] technique has emerged as a valuable approach to guide and structure the generation of content by LLMs. By utilizing a progressive hierarchical chain structure, researchers aim to enhance the coherence and contextuality of model-generated text [45, 53, 56]. This technique serves as a mechanism to direct the flow of information and ensure the generation of relevant and meaningful content [22, 47]. CoT play a crucial role in constraining the output of LLMs, enabling them to produce text that aligns closely with desired contexts and themes. Integrating the CoT technique with LLMs has the potential to improve the quality and relevance of generated text across a wide range of applications and use cases.

A key distinction of our approach from these methods is the use of generated context instead of pre-collected context during the inference step in CoA design. This allows us to fully leverage the inherent reasoning capabilities of LLMs. Additionally, our method employs a zero-shot approach during inference, making it adaptable across a range of LLM-based architectures.

3. Method

In this section, we provide a detailed description of the proposed method. We present the preliminary work related to our study in Section 3.1. Following this, we define the GSLs task and discuss two straightforward baseline approaches in Section 3.2. Finally, we provide a detailed explanation of our proposed Chain-of-Action method in Section 3.3.

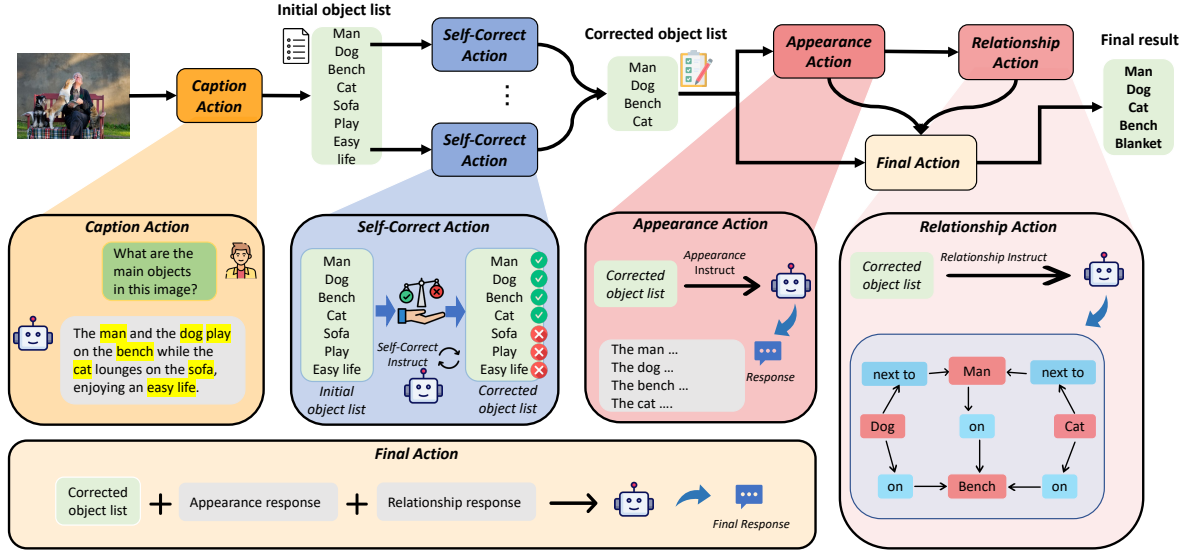


Figure 3. Pipeline of CoA. First, we utilize *Caption Action* to generate a comprehensive image description and extract an initial object list. *Self-Correct Action* refines this list, followed by *Appearance Action* and *Relationship Action* to capture detailed appearance features and relationships. Finally, we integrate these responses to create enriched context, guiding LMMs to achieve final semantic labels.

3.1. Preliminaries

VLM-based Image Classification. Let $\mathcal{X} \subset \mathbb{R}^d$ represent the d -dimensional image space, and $\mathcal{Y} = \{1, 2, \dots, k\}$ denote the label space with k distinct classes. VLM-based methods construct text prompts in the form of templates, such as “a photo of a $\{CLASS\}$ ”, where $CLASS$ is a placeholder for an element from \mathcal{Y} [34]. The text encoder in the VLM processes these templates to generate text embeddings, denoted as T . Simultaneously, for a given input image, the visual encoder maps the image into its corresponding visual embedding vector V . The core of VLM-based image classification lies in aligning the semantic spaces of V and T . VLM-based methods are typically trained on large-scale image-text datasets to learn a mapping function $f : \mathcal{X} \mapsto \mathcal{Y}$, where the objective is to match image representations to their corresponding textual labels. However, in standard VLM-based image classification, the label space \mathcal{Y} is manually pre-defined and fixed, which becomes impractical in the real-world scenarios where \mathcal{Y} is unknown and subject to continuous change.

Vocabulary-free Image Classification. Given the image space \mathcal{X} , Vocabulary-free Image Classification (VIC) aims to assign a class label y to a test image x without prior knowledge of the label set \mathcal{Y} [8]. Instead, VIC assumes access to a broader semantic class space \mathcal{S} (where $\mathcal{Y} \subset \mathcal{S}$), which encompasses all potential semantic concepts. The objective of VIC is to define a function f that maps an image to a semantic label within \mathcal{S} , i.e., $f : \mathcal{X} \mapsto \mathcal{S}$. However, the vastness of this semantic space presents a significant challenge, particularly when distinguishing fine-

grained concepts across diverse domains or handling long-tailed distributions. As such, this assumption often proves impractical in real-world applications.

3.2. Generative semantic labels

Task Definition. Given a test image $x_i \in \mathcal{X}$, Generative Semantic Labels (GSLs) aims to assign a semantic labels set Y_i to the test image x_i without prior knowledge of the label set \mathcal{Y} . Here, $Y_i \in \mathcal{C}$ is the set of relevant semantic labels associated with x_i , where $\mathcal{C} = 2^{\mathcal{S}}$. The goal of GSLs is to induce a map function $f : \mathcal{X} \mapsto 2^{\mathcal{S}}$. Notably, the key distinction between GSLs and VIC lies in the fact that GSLs assign multiple semantic labels to the test image x_i , rather than a single class label. Moreover, the VIC task requires additional methods to obtain a large semantic space \mathcal{S} and to retrieve the most relevant semantic label for a given test image. In contrast, GSLs does not rely on such assumptions, as \mathcal{S} is inherently the knowledge base of the LMMs, with the semantics derived solely from the model’s internal knowledge.

The primary challenge of the GSLs task lies in extracting the semantics of all entities within the test image. The core issue in method design is how to accomplish this without relying on predefined labels set or external semantic databases. Our only resource is the generalized knowledge embedded in LMMs. Therefore, fully leveraging the prior knowledge learned by these models during training becomes the most critical problem to solve in GSLs task. To address this, we can either directly extract entity semantics using the model’s image understanding capabilities or generate detailed textual descriptions via the captioning abili-

ties of LMMs, which can then be parsed for entity semantics. Based on this, we propose two straightforward baseline approaches: a single-stage method, using VQA-based LMMs to directly query the model for entity semantics, and a two-stage method, where captions are generated and then filtered to identify relevant entities, referred to as Caption-based LMMs.

VQA-based LMMs. Large Multimodal Models (LMMs) are powerful tools with human-competitive image understanding capabilities, capable of handling complex visual question-answering tasks. In this paper, we leverage this ability to extract high-quality entity semantics by fine-tuning LLaVA [29], a popular multimodal large model. We design various question templates to guide the model in generating the desired outputs (The detailed information regarding these question templates can be found in Appendix A). However, we observed that directly querying the model often yields suboptimal results. Specifically, the confidence scores for predicted labels tend to favor entities with particularly prominent features. Moreover, the generated labels frequently exhibit high semantic overlap, which is not aligned with the desired outcomes, as illustrated in Fig. 2.

Caption-based LMMs. To address the issue of semantic redundancy in VQA-based methods, we explore a captioning approach for the GSLs task. This involves first generating detailed image descriptions using LMMs, followed by filtering the captions to obtain the final set of entity semantics. The generated captions often capture fine-grained details, resulting in more comprehensive and diverse outputs. However, we observed that excessively long captions incur substantial computational cost, while shorter captions may overlook certain labels and ignore local details. This process requires significant parameter tuning to achieve optimal results. In addition, this approach is also constrained by the limitations of the filtering techniques. Since the image descriptions are generated based on the input image, the LMMs’ associative capabilities can lead to hallucinations, where the output includes entity semantics that do not accurately match the image content. As illustrated in Fig. 2, inadequate filtering may exacerbate this issue.

3.3. Chain-of-Action

Based on the analysis in the previous section, VQA-based LMMs struggle to produce ideal labels due to significant semantic overlap, while Caption-based LMMs face challenges with high parameter tuning costs, poor adaptability, and heavy reliance on filtering strategies. However, we observed that each interaction with LMMs provides valuable contextual information that can enhance the identification of target entities. Inspired by the success of Chain-of-Thought techniques in large language models and the application of In-context learning in multimodal tasks [15, 20, 32, 37], we propose a simple yet effective Chain-of-Action approach for

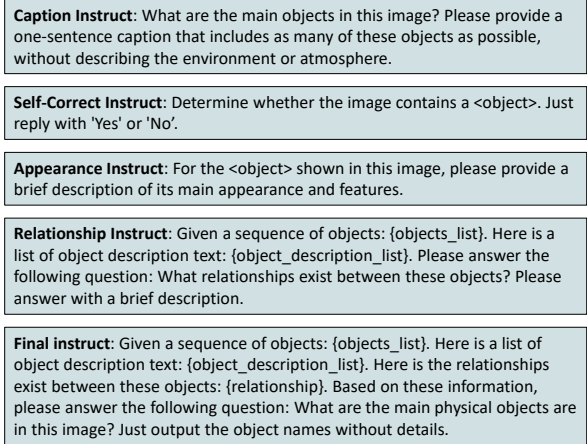


Figure 4. The instruction templates defined within the various action setting.

the GSLs task.

We define each interaction with LMMs as an individual action. By employing different combinations of prompts (as illustrated in Fig. 4), we interact with the LMMs to obtain complementary outputs. We establish a five-step process to guide the LMMs in producing: **(i) Caption Action:** Generate a one-sentence caption for the image and use a filtering strategy (detailed in the Appendix B) to extract an initial list of entities. **(ii) Utilize Self-Correct Action** to perform self-correction on each entity in the initial object list (isolating single-entity corrections improves instruction specificity, as LMMs handle Yes-or-No questions more effectively than open-ended What-and-How questions). **(iii) Apply Appearance Action** to extract each entity’s appearance and attributes. **(iv) Using Relationship Action,** infer relationships between entities by combining the corrected entity list with extracted appearance details. **(v) Employ Final Action** to integrate the entity list with outputs from *Appearance Action* and *Relationship Action*, generating the final entity list. To provide a comprehensive understanding of the proposed method, Fig. 3 illustrates the architecture and execution pipeline.

The proposed CoA method is capable of generating all relevant entity labels for an image without relying on predefined label sets or external database retrieval. The *Caption Action* step mitigates the issue of generating semantically redundant labels, while the *Self-Correct Action* ensures self-verification of the filtered labels, further unlocking the potential of LMMs. Additionally, the *Appearance Action* enhances the capture of local entity details, and the *Relationship Action* enriches the representation of inter-entity relationships, providing contextual depth for the Final Action. This progressive structure ensures that the LMMs’ output maintains high accuracy while improving the number of predicted entities. These findings are validated through ex-

Method	Split-0		Split-1		Split-2		Split-3		Avg		
	M _{clip} ↑	M _{ram} ↑	M _{clip} ↑	M _{ram} ↑	M _{clip} ↑	M _{ram} ↑	M _{clip} ↑	M _{ram} ↑	M _{clip} ↑	M _{ram} ↑	
VQA	BLIP-2 [24]	46.00	68.83	32.39	69.10	41.35	66.40	25.00	70.72	36.19	68.76
	InstructBLIP [9]	36.45	72.14	33.97	72.93	42.57	69.12	21.14	68.34	33.53	70.63
	LLaVA [29]	55.22	66.50	53.16	62.05	54.99	66.66	55.87	66.90	54.81	65.53
	MiniGPT-4 [58]	45.87	45.64	52.17	45.32	54.73	44.76	49.16	48.48	50.48	46.05
Caption	BLIP-2 [24]	64.45	69.87	55.27	70.03	66.58	72.57	36.74	69.12	55.76	70.40
	InstructBLIP [9]	69.37	69.12	69.69	70.54	73.44	72.08	71.04	74.05	70.89	71.48
	LLaVA [29]	58.88	60.16	66.06	65.28	63.62	67.93	67.21	65.57	63.94	64.74
	MiniGPT-4 [58]	46.76	40.34	52.98	37.32	52.09	39.62	45.30	43.63	49.28	40.23
CoA (Our)	81.23	75.18	79.83	78.54	84.51	79.69	84.23	76.54	82.45	77.49	

(a) Comparison of results on VOC.

Method	Split-0		Split-1		Split-2		Split-3		Avg		
	M _{clip} ↑	M _{ram} ↑	M _{clip} ↑	M _{ram} ↑	M _{clip} ↑	M _{ram} ↑	M _{clip} ↑	M _{ram} ↑	M _{clip} ↑	M _{ram} ↑	
VQA	BLIP-2 [24]	34.19	68.23	25.40	62.67	42.03	72.39	37.61	70.25	34.81	68.39
	InstructBLIP [9]	34.14	70.14	26.35	59.98	43.87	72.47	31.36	70.89	33.93	68.37
	LLaVA [29]	54.16	65.85	47.28	65.09	70.14	69.04	55.87	72.32	56.86	68.08
	MiniGPT-4 [58]	38.52	50.48	40.88	55.98	44.44	55.25	57.16	60.04	45.25	55.44
Caption	BLIP-2 [24]	60.17	62.35	41.00	65.65	62.79	64.76	58.70	72.66	55.67	66.36
	InstructBLIP [9]	64.73	75.20	61.08	72.78	61.91	77.44	63.00	71.71	62.68	74.28
	LLaVA [29]	67.67	63.29	67.63	66.84	75.42	75.96	69.61	71.70	70.08	69.45
	MiniGPT-4 [58]	44.28	45.26	39.60	49.69	47.66	51.60	58.99	51.52	47.63	49.52
CoA (Our)	77.70	82.04	78.60	80.37	84.20	83.02	82.90	76.51	80.85	80.49	

(b) Comparison of results on COCO.

Table 1. Comparison of results between the proposed CoA and various VQA-based and Caption-based methods in M_{clip} (%) and M_{ram} (%) metrics on the VOC and COCO datasets. The best performance is in bold.

Method	Split-0		Split-1		Split-2		Split-3		Avg		
	M _{clip} ↑	M _{ram} ↑	M _{clip} ↑	M _{ram} ↑	M _{clip} ↑	M _{ram} ↑	M _{clip} ↑	M _{ram} ↑	M _{clip} ↑	M _{ram} ↑	
VQA	BLIP-2 [24]	70.76	60.54	70.52	59.94	71.88	59.99	71.48	60.74	71.16	60.30
	InstructBLIP [9]	64.40	62.70	64.96	62.07	65.20	62.13	66.16	62.52	65.18	62.36
	LLaVA [29]	71.68	60.33	71.00	61.27	73.12	59.80	71.12	60.62	71.73	60.51
	MiniGPT-4 [58]	76.76	49.97	77.32	50.30	70.36	49.15	69.84	50.30	73.57	49.93
Caption	BLIP-2 [24]	72.68	63.01	70.92	61.98	73.08	62.31	73.36	62.56	72.51	62.47
	InstructBLIP [9]	72.24	65.73	72.88	66.15	72.76	64.98	72.12	65.57	72.50	65.61
	LLaVA [29]	74.76	61.71	73.32	63.77	75.08	61.21	72.44	63.80	73.90	62.62
	MiniGPT-4 [58]	77.84	43.62	78.00	43.98	73.80	44.40	71.36	44.06	75.25	44.02
CoA (Our)	89.30	70.43	84.70	70.99	87.70	70.23	87.50	68.57	87.30	70.06	

Table 2. Comparison of results between the proposed CoA and various VQA-based and Caption-based methods in M_{clip} (%) and M_{ram} (%) metrics on the NUS dataset. The best performance is in bold.

tensive experiments, as detailed in Section 4.

Dataset	# Split-0	# Split-1	# Split-2	# Split-3	# Total
VOC	1561	1775	1891	596	5823
COCO	29628	3583	4461	2465	40137
NUS	2500	2500	2500	2500	10000

Table 3. The details of datasets.

4. Experiment

In this section, we present an extensive overview of the datasets, models, baselines, implementation details and evaluation metrics utilized in all experiments (see Section 4.1). Furthermore, we provide extensive quantitative and

qualitative experiments in Sections 4.2 ~ 4.4 to validate the efficacy of the proposed method and compare its effectiveness to the existing state-of-the-art methods.

4.1. Setup

Datasets. The core of the GSLs task lies in identifying multiple entities within an image. To accurately assess the effectiveness of our approach, we employ widely used multi-label datasets for evaluation, including PASCAL VOC 2012 (VOC) [12], MS-COCO 2014 (COCO) [26], and NUS-WIDE (NUS) [7]. As our method operates in a zero-shot inference setting without training, we use only the test sets from these datasets. Specifically, following [4, 52], we divided each dataset into four non-overlapping subsets. For

Type	Split-0		Split-1		Split-2		Split-3		Avg	
	$M_{clip} \uparrow$	$M_{ram} \uparrow$	$M_{clip} \uparrow$	$M_{ram} \uparrow$	$M_{clip} \uparrow$	$M_{ram} \uparrow$	$M_{clip} \uparrow$	$M_{ram} \uparrow$	$M_{clip} \uparrow$	$M_{ram} \uparrow$
(i) LLaVA w/Action 5	67.65	74.64	67.38	76.89	75.15	75.54	65.77	74.27	68.99	75.34
(ii) LLaVA w/Action 1+5	79.24 (+11.59)	75.33 (+0.69)	77.86 (+10.48)	77.71 (+0.82)	73.02	78.79 (+3.25)	75.50 (+9.73)	75.53 (+1.26)	76.41 (+7.42)	76.84 (+1.50)
(iii) LLaVA w/Action 1+2+5	80.14 (+0.90)	75.56 (+0.23)	78.54 (+0.68)	78.29 (+0.58)	83.55 (+10.53)	79.01 (+0.22)	79.03 (+3.53)	75.23	80.32 (+3.91)	77.02 (+0.18)
(iv) LLaVA w/Action 1+2+3+5	79.63	75.84 (+0.28)	78.76 (+0.22)	78.28	83.66 (+0.11)	79.24 (+0.23)	80.54 (+1.51)	75.86 (+0.63)	80.65 (+0.33)	77.31 (+0.29)
(v) LLaVA w/Action 1+2+3+4+5(Our)	81.23 (+1.60)	75.18	79.83 (+1.07)	78.54 (+0.26)	84.51 (+0.85)	79.69 (+0.45)	84.23 (+3.69)	76.54 (+0.68)	82.45 (+1.80)	77.49 (+0.18)
Total \uparrow (Compared to (i))	(+13.58)	(+0.54)	(+12.45)	(+1.65)	(+9.36)	(+4.15)	(+18.46)	(+2.27)	(+13.46)	(+2.15)

Table 4. Comparison of various setting for CoA in M_{clip} (%) and M_{ram} (%) metrics on the VOC dataset. Due to page limitations, the *Caption Action*, *Self-Correct Action*, *Appearance Action*, *Relationship Action* and *Final Action* are abbreviated as Action 1 ~ 5.

Type	Split-0		Split-1		Split-2		Split-3		Avg	
	$M_{clip} \uparrow$	$M_{ram} \uparrow$	$M_{clip} \uparrow$	$M_{ram} \uparrow$	$M_{clip} \uparrow$	$M_{ram} \uparrow$	$M_{clip} \uparrow$	$M_{ram} \uparrow$	$M_{clip} \uparrow$	$M_{ram} \uparrow$
LLaVA-1.5-7B	55.22	66.50	53.16	62.05	54.99	66.66	55.87	66.9	54.81	65.53
LLaVA-1.5-7B w/ CoA	81.23 (+26.01)	75.18 (+8.68)	79.83 (+26.67)	78.54 (+16.49)	84.51 (+29.52)	79.69 (+13.03)	84.23 (+28.36)	76.54 (+9.64)	82.45 (+27.64)	77.49 (+11.96)
LLaVA-1.5-13B	68.74	69.67	68.34	67.77	77.95	66.39	68.62	68.5	70.91	68.08
LLaVA-1.5-13B w/ CoA	81.42 (+12.68)	76.94 (+7.27)	81.63 (+13.29)	79.72 (+11.95)	86.94 (+9.99)	84.35 (+17.96)	90.76 (+22.14)	79.70 (+11.20)	85.19 (+14.28)	80.18 (+12.10)

Table 5. Comparison of various LMMs with CoA in M_{clip} (%) and M_{ram} (%) metrics on the VOC dataset. The best performance is in bold.

the NUS dataset, we validate our method’s effectiveness on a test set created by randomly sampling 10,000 images from the original NUS test set. The more details of these datasets can be obtained from Table 3 and Appendix E.

Models. The pre-trained LLaVA-1.5-7B [29] model is used as the base model, and we apply our CoA approach to this model to address GSLs tasks. Furthermore, we compare our approach with three popular LMMs: BLIP-2 [24], InstructBLIP [9], and MiniGPT-4 [58]. Additional details are provided in Appendix C.

Baselines. We categorize our baselines into two main groups for comparative analysis. The first group involves using VQA models to directly predict class names associated with an image. This includes BLIP-2 [24], InstructBLIP [9], LLaVA [29], and MiniGPT-4 [58], all of which have demonstrated outstanding performance in VQA tasks. The second group consists of captioning approaches, as captions effectively encapsulate the semantic content of images. For these, we also evaluate the same four LMMs, given their proven efficacy in caption generation.

Implementation Details. All experiments were conducted on two NVIDIA 4090 GPUs. Following CaSED [8] and the BLIP-2 [24] demo, for captioning, we used the prompt “Question: what’s in the image? Answer:”. For VQA, we used the prompt “Question: What are the names of objects in this image? Answer:”.

Evaluation metrics. Given that the GSLs task requires identifying multiple entities, we aim for model predictions to be as comprehensive and accurate as possible. Therefore, we designed two evaluation metrics that separately assess comprehensiveness (M_{clip}) and accuracy (M_{ram}). Due to page limitations, we provide details on the definitions and calculation formulas for these two metrics in Appendix D.

4.2. Quantitative results

Comprehensive performance results for CoA and the baseline methods are detailed in Table 1 and Table 2 for both M_{clip} (%) and M_{ram} (%). Our proposed method consistently surpasses all baselines across all evaluation metrics and datasets. Notably, (1) CoA exceeds the second-best method by an average of +11.56% in M_{clip} and +6.01% in M_{ram} on the VOC dataset; (2) it demonstrates a +10.77% average improvement in M_{clip} and +6.21% in M_{ram} on the COCO dataset; and (3) it surpasses the second-best method by +13.4% in M_{clip} and +4.45% in M_{ram} on the NUS dataset. These results highlight the effectiveness of CoA, achieving the best performance both in terms of semantic comprehensiveness and accuracy of predicted labels.

An interesting observation from the table is that overall, VQA-based approaches perform less effectively than caption-based methods in M_{clip} . This is primarily because the GSLs task emphasizes identifying all entities relevant to an image. Single-question VQA interactions often lead LMMs to focus on specific local details within an image, whereas captioning guides the model to capture a more comprehensive set of features, resulting in outputs that encompass all relevant entities. This insight influenced the design of our action chain, where the first action is dedicated to obtaining a broad image description. Our experiments validate the effectiveness of this setup.

4.3. Effectiveness analysis of CoA

To validate the effectiveness of the CoA, we decomposed it into multiple independent components. Since Action 5 serves as the primary step for the GSLs task, responsible for identifying all entity labels in the test image, we used it as the baseline. We then incrementally added each subsequent component to the CoA and evaluated the performance

Type	Split-0		Split-1		Split-2		Split-3		Avg	
	M _{clip} ↑	M _{ram} ↑	M _{clip} ↑	M _{ram} ↑	M _{clip} ↑	M _{ram} ↑	M _{clip} ↑	M _{ram} ↑	M _{clip} ↑	M _{ram} ↑
CoA	81.23	75.18	79.83	78.54	84.51	79.69	84.23	76.54	82.45	77.49
Single Interaction	65.86 (-15.37)	49.18 (-26.00)	62.42 (-17.41)	39.89 (-38.65)	71.44 (-13.07)	42.79 (-36.90)	67.28 (-16.95)	36.97 (-39.57)	66.75 (-15.70)	42.21 (-35.28)

Table 6. Comparison of multiple interaction (CoA) with single interaction in M_{clip} (%) and M_{ram} (%) metrics on the VOC dataset.

impact after each addition. The results of these evaluations are shown in Table 4. From Table 4, it is evident that each added component contributes to significant improvements in both M_{clip} and M_{ram} metrics. Notably, the complete action chain outperforms using only Action 5, achieving an increase of +13.46% in the M_{clip} metric and +2.15% in the M_{ram} metric. These findings strongly highlight the performance enhancements brought by the CoA, which proves the effectiveness of the proposed method.

4.4. Applicability for various LMMs

To evaluate the adaptability of CoA across various LMMs, we conducted experiments by changing the base model and testing its performance on different LMMs. Specifically, we employed LLaVA-1.5-7B and LLaVA-1.5-13B as base model. Although LLaVA-1.5-13B is generally more capable than LLaVA-1.5-7B, integrating CoA with LLaVA-1.5-13B still resulted in significant improvements. Notably, there was an increase of +14.28% in the M_{clip} metric and +12.1% in the M_{ram} metric. These findings demonstrate the adaptability and effectiveness of the proposed CoA across diverse LMMs, highlighting its capability to integrate seamlessly with different model architectures.

4.5. Additional ablations study

Multiple interaction vs single interaction. To validate the advantage of multiple interactions, we designed an experiment inspired by the concept of In-Context Learning. This involved merging the multiple actions of CoA into a single interaction (i.e., guiding LMMs to simultaneously consider captions, the appearance of entities, and relationships between entities within a single interaction; the detailed merged template is provided in Appendix F). The comparison of single-interaction performance versus multi-interaction CoA is reported in Table 6. The results clearly demonstrate that multiple interactions provide significant performance benefits over a single-step approach, attributed to the more granular processing and well-defined task objectives that facilitate more accurate outputs from LMMs.

Time cost of CoA. Given that the proposed CoA method involves multiple interactions with LMMs, it is essential to evaluate the time cost associated with the overall execution process. We analyze the computational efficiency of CoA versus VQA-based LMMs and Caption-based LMMs and report their inference time in Table 7. Notably, our approach maintains a comparable execution efficiency despite multi-

ple interactions. This is attributed to the simplicity of each individual interaction, ensuring that the total inference time remains within an acceptable range.

Method		Inference time (ms) ↓
VQA	BLIP-2 [24]	6650 ± 117
	LLaVA-1.5 [29]	753 ± 14
	MiniGPT-4 [58]	11216 ± 335
Caption	BLIP-2 [24]	6870 ± 177
	LLaVA-1.5 [29]	3073 ± 152
	MiniGPT-4 [58]	14760 ± 1433
CoA (Our)		6110 ± 149

Table 7. Computational cost of different methods on the Split-3 of VOC dataset.

With / Without Ram filtering. During the experimental process, we observed that beyond using the RAM model for designing evaluation metrics, its confidence scores could also be leveraged to filter generated targets. To validate this, we conducted experiments comparing results with and without RAM-based filtering, as reported in Table 8. The results demonstrate that applying this filtering method significantly improves the accuracy of the GSLs task.

Dataset	Method	Split-0	Split-1	Split-2	Split-3	Avg
VOC	CoA	75.18	78.54	79.69	76.54	77.49
	CoA w/ filter	88.19	88.84	89.64	88.25	88.73
COCO	CoA	82.04	80.37	83.02	76.51	80.49
	CoA w/ filter	91.88	91.03	93.79	88.32	91.11
NUS	CoA	70.43	70.99	70.23	68.57	70.06
	CoA w/ filter	84.94	84.93	84.39	83.67	84.46

Table 8. Comparison of CoA without / with RAM filtering in M_{ram} metric on VOC dataset.

5. Conclusion

In this work, unlike traditional VLMs that rely on predefined label sets, we propose a new task, GSLs, which generate comprehensive and contextually relevant labels from an unconstrained semantic space. Besides, we introduced an innovative Chain-of-Action (CoA) method designed to handle the challenging GSLs task. By breaking down the generative task into sequential actions that iteratively extract and refine key information, our method ensures that LMMs generate more accurate and complete semantic labels. Finally, extensive evaluations on widely-used benchmark datasets validate the efficacy of CoA, showcasing significant performance gains across multiple key metrics. This highlights

the potential of our method to improve label generation in dynamic, evolving environments.

A. Instruction templates of VQA LMMs

In this section, we present several instruction templates used within the VQA-based LMMs baselines, as illustrated in Fig. 5. For our study, these templates were employed to directly obtain semantic labels present in the images when applying the VQA-based baseline methods. We evaluated the effectiveness of these different instruction templates and selected the optimal configuration for comparison. The results of these comparisons are reported in Table 1 and Table 2 in the main manuscript.

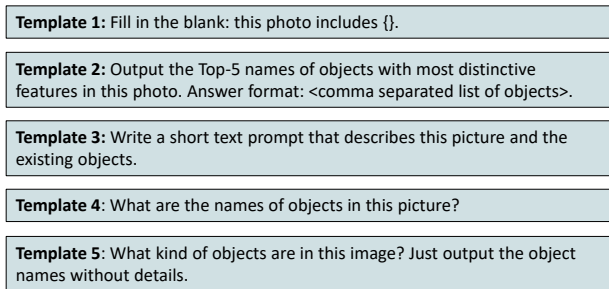


Figure 5. The instruction templates of VQA LMMs.

B. Details of filtering strategy

In this section, we provide additional details on how to filter the initial list of semantic labels after performing the *Caption Action*. For simplicity and efficiency, we adopt a straightforward approach. Specifically, we first create a set of all words present in the generated caption. This set is then filtered step by step. Using the *inflect* package, we perform part-of-speech tagging to identify and retain only noun-type semantic labels. Finally, we remove irrelevant entries (e.g., “image,” “photo,” “logo,” etc.) that are unrelated to the GSLs task, and then apply deduplication and singular/plural normalization. It is worth noting that this filtering strategy is a basic, streamlined process, and it is applied consistently across all Caption-based LMMs baseline methods.

C. Details for the models

In this section, we provide a detailed description of the various LMMs employed in the baseline methods. The specific details are outlined as follows.

- **LLaVA-1.5.** The LLaVA [29] architecture stands out as a state-of-the-art (SOTA) LMM method, notable for its effective integration of CLIP visual features and LLM

language tokens through a straightforward linear projection into a shared embedding space. LLaVA is fine-tuned using the LLaVA-Instruct-158k dataset, which consists of images paired with conversational prompts, detailed descriptions, and complex reasoning responses, achieving superior visual alignment compared to basic image-text pairs. In this study, we evaluate LLaVA-1.5 [29], an enhanced version that offers improved baselines. Key advancements over the original model include: (1) replacing the linear projection with a multi-layer perceptron (MLP) and (2) pretraining on a more diverse set of datasets.

- **BLIP-2.** BLIP-2 [24] is an advanced vision-language model designed to bridge the gap between visual and linguistic representations by incorporating a two-stage learning framework. The model begins by using a lightweight visual encoder (such as CLIP [34]) to extract image features, followed by a query-based cross-modal transformer that effectively aligns these visual representations with text. This architecture allows BLIP-2 to perform zero-shot and few-shot learning tasks with enhanced efficiency and scalability. By leveraging pre-training strategies that integrate visual context with language models like OPT or GPT-style backbones, BLIP-2 achieves strong performance in both image-to-text and multimodal tasks. Its innovative design reduces the computational overhead of extensive vision-language alignment training, making it a competitive choice for tasks requiring detailed image understanding and nuanced text generation.
- **InstructBLIP.** InstructBLIP [9] is a cutting-edge vision-language model designed to align multimodal understanding with human-like instruction following. The architecture builds upon the foundation of BLIP-2 [24], integrating a vision encoder (e.g., CLIP [34]) with an enhanced cross-modal transformer that incorporates instruction-based pretraining. InstructBLIP distinguishes itself by being fine-tuned with a diverse range of multimodal instructions, enabling the model to better understand and respond to complex tasks that involve visual and textual cues. This enables more coherent and contextually relevant responses, aligning model outputs with user prompts across various scenarios, from question-answering and image captioning to reasoning and complex interactions. By incorporating instruction-tuned objectives, InstructBLIP advances performance in both zero-shot and fine-tuned benchmarks, demonstrating superior adaptability and alignment with user intent compared to standard vision-language models.
- **MiniGPT-4.** MiniGPT-4 [58] is a vision-language model designed to emulate the capabilities of large multimodal models, such as GPT-4 [1], while being more lightweight and efficient. It integrates a visual encoder,

typically based on advanced vision transformers like CLIP [34], with a language model through a linear transformation layer, aligning visual embeddings with language tokens. MiniGPT-4 undergoes a two-stage training process: first, a pretraining phase using image-text pairs to establish a foundational understanding of multimodal data, and second, an instruction-tuning phase to refine its responses and better align them with human interactions. This instruction-tuned process enhances the model’s performance on tasks that involve image descriptions, visual question answering, and complex reasoning. MiniGPT-4 is notable for its reduced computational requirements while maintaining strong alignment and contextual comprehension capabilities, making it a practical alternative for applications requiring efficient multimodal reasoning.

D. Evaluation metrics

Given that the GSC task requires identifying multiple entities, we aim for model predictions to be as comprehensive and accurate as possible. Therefore, we designed two evaluation metrics that separately assess these aspects. Specifically, leveraging the generalization capability of the CLIP model, we used the prompt P_{com} : “This image contains [...]” to capture the comprehensiveness of predicted entities. Next, given the predicted entity list Y_i and the manually annotated entity list \bar{Y}_i , we compute their respective similarities to the image. Then, we can obtain the comprehensive score CS_i or the predicted labels of each test image I_i from the following formula:

$$CS_i = \mathbf{1} [\cos\langle T(P_{com}(Y_i)), V(I_i) \rangle > \cos\langle T(P_{com}(\bar{Y}_i)), V(I_i) \rangle], \quad (1)$$

where $\mathbf{1}[\cdot]$ denotes the indicator function, $T(\cdot)$ and $V(\cdot)$ denotes the text and image encoder of CLIP model. A prediction is scored only if the similarity of the model-generated prompt exceeds that of the prompt based on manual annotations. Here, we utilize the label set provided by the dataset itself as the manual-annotated labels. Then, we can obtain the $M_{clip} = \sum_i^N CS_i/N$ to assess the coverage of predicted labels, where N denotes the number of test images.

To evaluate the accuracy of each predicted label, we leverage the RAM model to score each predicted entity label. RAM, a large-scale multi-label model trained on extensive multi-label datasets, has demonstrated significant recognition accuracy in multi-label tasks. Given a test image and a set of labels, RAM calculates a confidence score for each label in the list, filtering out labels that align with the image based on confidence thresholds. The accuracy score AS_i of the predicted label list is then computed using the following formula:

$$AS_i = \text{Sigmod}(\sum_j^L H(RAM(Y_i^j))), \quad (2)$$

where $RAM(Y_i^j)$ denotes the confidence score calculated by RAM model for the label j from predicted labels set Y_i , L denotes the number of Y_i , and

$$H(RAM(Y_i^j)) = \begin{cases} 1 & \text{if } RAM(Y_i^j) \geq \sigma \\ -1 & \text{if } RAM(Y_i^j) < \sigma \end{cases}, \quad (3)$$

where σ denotes the threshold of confidence score. Following the RAM configuration, we set the confidence threshold to 0.73. A straightforward scoring rule is applied: one point is added for each correct prediction, and one point is subtracted for each incorrect prediction. Finally, we calculate the $M_{ram} = \sum_i^N AS_i/N$ to assess the accuracy of the predicted labels.

E. Details for the datasets

We employ widely used datasets for evaluation, including PASCAL VOC 2012 (VOC) [12], MS-COCO 2014 (COCO) [26], and NUS-WIDE (NUS) [7]. The more details of these datasets are outlined as follows.

- **PASCAL VOC 2012 (VOC)** [12]: The PASCAL VOC 2012 dataset is a benchmark for evaluating algorithms in visual object recognition and detection. It is part of the PASCAL Visual Object Classes Challenge, a series of competitions designed to push the boundaries of object detection and classification research. The dataset comprises 20 object categories spanning everyday scenes, such as vehicles, animals, and household items. It includes a training/validation set with over 11,000 annotated images and approximately 27,000 object instances, providing a robust foundation for developing and benchmarking algorithms. Each image in the dataset is annotated with high-quality, pixel-wise segmentation masks and object bounding boxes, enabling multi-task learning in both image classification and semantic segmentation. VOC remains widely used due to its diverse visual content, standardized evaluation metrics, and significant influence on advancing deep learning methods in computer vision. Source: <http://host.robots.ox.ac.uk/pascal/VOC/>
- **MS-COCO 2014 (COCO)** [26]: The MS-COCO 2014 dataset is a widely recognized benchmark in the computer vision community, designed to facilitate research in object detection, segmentation, and captioning. It contains over 300,000 images with rich contextual information, depicting 80 object categories commonly found in everyday scenes. The dataset is meticulously annotated, featuring more than 2.5 million labeled instances that include precise object boundaries and segmentation masks, enabling comprehensive multi-task learning. In addition to detection and segmentation tasks, COCO provides a unique image captioning component, where each image is paired with multiple human-generated

descriptions to support advancements in image-to-text models. Its diverse and challenging set of images, captured in realistic and complex environments, has made COCO a cornerstone for training and evaluating modern deep learning algorithms, significantly influencing state-of-the-art performance in visual understanding tasks. Source: <http://images.cocodataset.org/zips/val2014.zip>

- **NUS-WIDE (NUS)** [7]: The NUS-WIDE dataset is an extensive benchmark designed to facilitate research in large-scale image classification, multi-label annotation, and retrieval. NUS comprises over 260,000 images sourced from Flickr, annotated with 81 concept labels spanning various categories such as objects, scenes, and events. Each image in the dataset is tagged with one or more labels, supporting multi-label learning and evaluation. The annotations are derived using both automated and manual verification processes, ensuring label reliability and diversity. NUS also includes pre-extracted low-level visual features, providing a foundation for baseline experiments. This dataset is notable for its real-world distribution, reflecting the challenges of noisy data and varying image quality found in online media. Its breadth and comprehensive labeling make it a valuable resource for advancing multi-label classification, image retrieval, and large-scale visual recognition research.

F. Merged template for single interaction

To thoroughly validate the advantages offered by multiple interactions, we designed an experiment based on the principles of In-Context Learning [15, 32]. In this experiment, the sequential steps of the proposed CoA framework were combined into a single interaction. This approach guided the LMMs to concurrently process captions, entity appearances, and inter-entity relationships, enabling them to consider all relevant aspects within a unified inference step. This consolidated approach aimed to explore the trade-off between a single, comprehensive interaction and the progressive, step-by-step nature of CoA. The specific structure and details of the merged template used for this experiment are illustrated in Fig. 6.

Single instruction template:
 For the provided image, please consider the following aspects and respond to the final question:

1. Objects that are relevant to answering the question.
2. Object attributes that are relevant to answering the question.
3. Object relationships that are relevant to answering the question.

Question: What are the main physical objects are in this image?
 Just output the object names without details.

Figure 6. The merged template for single interaction.

G. Additional comparative results

In this section, we present additional comparative results under various settings, including LLaVA-VQA, LLaVA-Caption, Human-labeled, and the proposed CoA. Here, the label set provided by the dataset itself is treated as the Human-labeled labels. The comparative results are illustrated in Fig. 7 and Fig. 8.

For each setting, we compare the predicted labels, calculate the number of correct predictions, and highlight these counts with green numbers. As shown in Fig. 4 and Fig. 5, both LLaVA-VQA and LLaVA-Caption, as well as Human-labeled annotations, tend to focus on predicting prominent features. However, due to the subjectivity of human annotators and the ambiguity in the goal of single-interaction models, these methods result in fewer predicted labels and lower accuracy compared to our proposed CoA. These findings underscore the effectiveness of our approach, which leverages multi-step interactions to achieve more precise and comprehensive semantic label predictions.

References

- [1] Josh Achiam, Steven Adler, Sandhini Agarwal, Lama Ahmad, Ilge Akkaya, Florencia Leoni Aleman, Diogo Almeida, Janko Altenschmidt, Sam Altman, Shyamal Anadkat, et al. Gpt-4 technical report. *arXiv preprint arXiv:2303.08774*, 2023. 1, 3, 9
- [2] Jean-Baptiste Alayrac, Jeff Donahue, Pauline Luc, Antoine Miech, Iain Barr, Yana Hasson, Karel Lenc, Arthur Mensch, Katherine Millican, Malcolm Reynolds, et al. Flamingo: a visual language model for few-shot learning. *Advances in Neural Information Processing Systems*, 35:23716–23736, 2022. 3
- [3] Stanislaw Antol, Aishwarya Agrawal, Jiasen Lu, Margaret Mitchell, Dhruv Batra, C Lawrence Zitnick, and Devi Parikh. Vqa: Visual question answering. In *Proceedings of the IEEE International Conference on Computer Vision*, pages 2425–2433, 2015. 1, 3
- [4] Amir Bar, Yossi Gandelsman, Trevor Darrell, Amir Globerson, and Alexei A. Efros. Visual prompting via image inpainting. In *Proceedings of Annual Conference on Neural Information Processing Systems*, 2022. 6
- [5] Maciej Besta, Nils Blach, Ales Kubicek, Robert Gerstenberger, Michal Podstawski, Lukas Gianinazzi, Joanna Gajda, Tomasz Lehmann, Hubert Niewiadomski, Piotr Nyczyk, et al. Graph of thoughts: Solving elaborate problems with large language models. In *Proceedings of the AAAI Conference on Artificial Intelligence*, pages 17682–17690, 2024. 3
- [6] Tom B. Brown, Benjamin Mann, Nick Ryder, Melanie Subbiah, Jared Kaplan, Prafulla Dhariwal, Arvind Neelakantan, Pranav Shyam, Girish Sastry, Amanda Askell, Sandhini Agarwal, Ariel Herbert-Voss, Gretchen Krueger, Tom Henighan, Rewon Child, Aditya Ramesh, Daniel M. Ziegler, Jeffrey Wu, Clemens Winter, Christopher Hesse, Mark Chen, Eric Sigler, Mateusz Litwin, Scott Gray, Benjamin Chess,

	 incorrect label	 correct label										
												
LLaVA-VQA	Jump	✗	1	Dog	✓	2	Bicycle	✓	2	Hat	✓	3
	Horse	✓		Speaker	✗		backpack	✗		Horse	✓	
	Fence	✗		Couch	✓		Helmet	✓		Fence	✓	
LLaVA-Caption	Girl	✓	3	Couch	✓	4	Helmet	✓	2	Women	✓	2
	Horse	✓		Man	✓		Bicycle	✓		Horse	✓	
	Fence	✓		Dog	✓							
				Floor	✓							
Human-labeled	Person	✓	2	Person	✓	3	Person	✓	3	Person	✓	2
	Horse	✓		Dog	✓		Bicycle	✓		Horse	✓	
				Sofa	✓		Potted plant	✓				
CoA (Our)	Person	✓	4	Dog	✓	4	Man	✓	5	Women	✓	4
	Jacket	✓		Man	✓		Bicycle	✓		Horse	✓	
	Barrier	✓		Couch	✓		Helmet	✓		Straw hat	✓	
	Horse	✓		Floor	✓		Building	✓		Fence	✓	
							Potted plant	✓				

Figure 7. Comparison of various settings, including LLaVA-VQA, LLaVA-Caption, Human-labeled and the proposed CoA method. The numbers annotated in the figure represent the count of correctly predicted semantic labels.

	 incorrect label	 correct label										
												
LLaVA-VQA	Person	✓	3	Monitor	✓	3	Truck	✓	3	toothbrush	✓	2
	Horse	✓		Mouse	✓		Pole	✗		toothpaste	✓	
	Bag	✓		Cup	✗		Fence	✓				
				Desk	✓		Train	✓				
LLaVA-Caption	Child	✓	4	Desk	✓	3	Train	✓	2	Care item	✗	2
	Field	✓		Office	✗		Track	✓		Toothbrush	✓	
	Horse	✓		Chair	✓					Toothpaste	✓	
	Man	✓		Computer	✓							
Human-labeled	Person	✓	3	Chair	✓	3	Person	✓	3	Toothbrush	✓	1
	Horse	✓		TV	✓		Train	✓				
	Coa	✓		Vase	✓		Truck	✓				
CoA (Our)	Man	✓	6	Computer	✓	7	Train	✓	7	Toothpaste	✓	3
	Child	✓		Desk	✓		Truck	✓		Toothbrush	✓	
	Horse	✓		Keyboard	✓		Building	✓		mouthwash	✓	
	Saddle	✓		Chair	✓		Traffic light	✓				
	Bag	✓		Monitor	✓		Fence	✓				
	Cow	✓		Mouse	✓		Track	✓				
				Potted plant	✓		Tree	✓				

Figure 8. Comparison of various settings, including LLaVA-VQA, LLaVA-Caption, Human-labeled and the proposed CoA method. The numbers annotated in the figure represent the count of correctly predicted semantic labels.

- Jack Clark, Christopher Berner, Sam McCandlish, Alec Radford, Ilya Sutskever, and Dario Amodei. Language models are few-shot learners. In *Proceedings of Annual Conference on Neural Information Processing Systems*, 2020. [3](#)
- [7] Tat-Seng Chua, Jinhui Tang, Richang Hong, Haojie Li, Zhiping Luo, and Yantao Zheng. Nus-wide: a real-world web image database from national university of singapore. In *Proceedings of the ACM international conference on image and video retrieval*, pages 1–9, 2009. [6](#), [10](#), [11](#)
- [8] Alessandro Conti, Enrico Fini, Massimiliano Mancini, Paolo Rota, Yiming Wang, and Elisa Ricci. Vocabulary-free image classification. In *Proceedings of Annual Conference on Neural Information Processing Systems*, 2023. [1](#), [4](#), [7](#)
- [9] Wenliang Dai, Junnan Li, Dongxu Li, Anthony Meng Huat Tiong, Junqi Zhao, Weisheng Wang, Boyang Li, Pascale Fung, and Steven C. H. Hoi. Instructblip: Towards general-purpose vision-language models with instruction tuning. In *Proceedings of Advances in Neural Information Processing Systems*, 2023. [1](#), [3](#), [6](#), [7](#), [9](#)
- [10] Danny Driess, Fei Xia, Mehdi S. M. Sajjadi, Corey Lynch, Aakanksha Chowdhery, Brian Ichter, Ayzaan Wahid, Jonathan Tompson, Quan Vuong, Tianhe Yu, Wenlong Huang, Yevgen Chebotar, Pierre Sermanet, Daniel Duckworth, Sergey Levine, Vincent Vanhoucke, Karol Hausman, Marc Toussaint, Klaus Greff, Andy Zeng, Igor Mordatch, and Pete Florence. Palm-e: An embodied multimodal language model. In *Proceedings of International Conference on Machine Learning*, pages 8469–8488, 2023. [3](#)
- [11] Zhengxiao Du, Yujie Qian, Xiao Liu, Ming Ding, Jiezhong Qiu, Zhilin Yang, and Jie Tang. GLM: general language model pretraining with autoregressive blank infilling. In *Proceedings of Annual Meeting of the Association for Computational Linguistics*, pages 320–335, 2022. [3](#)
- [12] M Everingham, L Van Gool, CKI Williams, J Winn, and A Zisserman. The pascal visual object classes challenge 2012 (voc2012) results. 2012 <http://www.pascal-network.org/challenges>. In *VOC/voc2012/workshop/index.html*, 2012. [6](#), [10](#)
- [13] Kaituo Feng, Changsheng Li, Dongchun Ren, Ye Yuan, and Guoren Wang. On the road to portability: Compressing end-to-end motion planner for autonomous driving. In *Proceedings of the IEEE/CVF Conference on Computer Vision and Pattern Recognition*, pages 15099–15108, 2024. [1](#)
- [14] Zipeng Fu, Ashish Kumar, Ananye Agarwal, Haozhi Qi, Jitendra Malik, and Deepak Pathak. Coupling vision and proprioception for navigation of legged robots. In *Proceedings of the IEEE/CVF Conference on Computer Vision and Pattern Recognition*, pages 17252–17262, 2022. [1](#)
- [15] Xiang Gao and Kamalika Das. Customizing language model responses with contrastive in-context learning. In *Proceedings of the AAAI Conference on Artificial Intelligence*, pages 18039–18046, 2024. [5](#), [11](#)
- [16] Shashank Goel, Hritik Bansal, Sumit Bhatia, Ryan Rossi, Vishwa Vinay, and Aditya Grover. Cyclip: Cyclic contrastive language-image pretraining. *Advances in Neural Information Processing Systems*, 35:6704–6719, 2022. [1](#), [3](#)
- [17] Kaiming He, Haoqi Fan, Yuxin Wu, Saining Xie, and Ross Girshick. Momentum contrast for unsupervised visual representation learning. In *Proceedings of the IEEE/CVF Conference on Computer Vision and Pattern Recognition*, pages 9729–9738, 2020. [3](#)
- [18] Drew A Hudson and Christopher D Manning. Gqa: A new dataset for real-world visual reasoning and compositional question answering. In *Proceedings of the IEEE/CVF Conference on Computer Vision and Pattern Recognition*, pages 6700–6709, 2019. [1](#)
- [19] Chao Jia, Yinfei Yang, Ye Xia, Yi-Ting Chen, Zarana Parekh, Hieu Pham, Quoc Le, Yun-Hsuan Sung, Zhen Li, and Tom Duerig. Scaling up visual and vision-language representation learning with noisy text supervision. In *Proceedings of International Conference on Machine Learning*, pages 4904–4916. PMLR, 2021. [3](#)
- [20] Ryuto Koike, Masahiro Kaneko, and Naoaki Okazaki. OUTFOX: llm-generated essay detection through in-context learning with adversarially generated examples. In *Proceedings of the AAAI Conference on Artificial Intelligence*, pages 21258–21266. [5](#)
- [21] Takeshi Kojima, Shixiang Shane Gu, Machel Reid, Yutaka Matsuo, and Yusuke Iwasawa. Large language models are zero-shot reasoners. In *Proceedings of Annual Conference on Neural Information Processing Systems*, 2022. [2](#)
- [22] Bin Lei, Chunhua Liao, Caiwen Ding, et al. Boosting logical reasoning in large language models through a new framework: The graph of thought. *arXiv preprint arXiv:2308.08614*, 2023. [3](#)
- [23] Junnan Li, Dongxu Li, Caiming Xiong, and Steven Hoi. Blip: Bootstrapping language-image pre-training for unified vision-language understanding and generation. In *Proceedings of International Conference on Machine Learning*, pages 12888–12900. PMLR, 2022. [1](#), [3](#)
- [24] Junnan Li, Dongxu Li, Silvio Savarese, and Steven Hoi. Blip-2: Bootstrapping language-image pre-training with frozen image encoders and large language models. In *Proceedings of International Conference on Machine Learning*, pages 19730–19742. PMLR, 2023. [1](#), [3](#), [6](#), [7](#), [8](#), [9](#)
- [25] Zengsheng Liang, Zhong Chen, Qisen Wu, Xinyi Gao, and Xianmin Zhang. Precision alignment in cell microinjection based on hybrid triple-view micro-vision. *IEEE Trans. Robotics*, 40:158–171, 2024. [1](#)
- [26] Tsung-Yi Lin, Michael Maire, Serge Belongie, James Hays, Pietro Perona, Deva Ramanan, Piotr Dollár, and C Lawrence Zitnick. Microsoft coco: Common objects in context. In *Computer Vision—ECCV 2014: 13th European Conference, Zurich, Switzerland, September 6–12, 2014, Proceedings, Part V 13*, pages 740–755. Springer, 2014. [6](#), [10](#)
- [27] Haotian Liu, Kilho Son, Jianwei Yang, Ce Liu, Jianfeng Gao, Yong Jae Lee, and Chunyuan Li. Learning customized visual models with retrieval-augmented knowledge. In *Proceedings of the IEEE/CVF Conference on Computer Vision and Pattern Recognition*, pages 15148–15158, 2023. [1](#)
- [28] Haotian Liu, Chunyuan Li, Yuheng Li, and Yong Jae Lee. Improved baselines with visual instruction tuning. In *Proceedings of the IEEE/CVF Conference on Computer Vision and Pattern Recognition*, pages 26296–26306, 2024. [3](#)
- [29] Haotian Liu, Chunyuan Li, Qingyang Wu, and Yong Jae Lee.

- Visual instruction tuning. *Advances in Neural Information Processing Systems*, 36, 2024. 1, 3, 5, 6, 7, 8, 9
- [30] Kenneth Marino, Mohammad Rastegari, Ali Farhadi, and Roozbeh Mottaghi. Ok-vqa: A visual question answering benchmark requiring external knowledge. In *Proceedings of the IEEE/CVF Conference on Computer Vision and Pattern Recognition*, pages 3195–3204, 2019. 3
- [31] Chancharik Mitra, Brandon Huang, Trevor Darrell, and Roei Herzig. Compositional chain-of-thought prompting for large multimodal models. In *Proceedings of IEEE/CVF Conference on Computer Vision and Pattern Recognition*, pages 14420–14431, 2024. 2
- [32] Zhijie Nie, Richong Zhang, Zhongyuan Wang, and Xudong Liu. Code-style in-context learning for knowledge-based question answering. In *Proceedings of the AAAI Conference on Artificial Intelligence*, pages 18833–18841, 2024. 5, 11
- [33] Alec Radford, Jeffrey Wu, Rewon Child, David Luan, Dario Amodei, Ilya Sutskever, et al. Language models are unsupervised multitask learners. *OpenAI blog*, 1(8):9, 2019. 3
- [34] Alec Radford, Jong Wook Kim, Chris Hallacy, Aditya Ramesh, Gabriel Goh, Sandhini Agarwal, Girish Sastry, Amanda Askell, Pamela Mishkin, Jack Clark, et al. Learning transferable visual models from natural language supervision. In *Proceedings of International Conference on Machine Learning*, pages 8748–8763. PMLR, 2021. 1, 3, 4, 9, 10
- [35] Colin Raffel, Noam Shazeer, Adam Roberts, Katherine Lee, Sharan Narang, Michael Matena, Yanqi Zhou, Wei Li, and Peter J Liu. Exploring the limits of transfer learning with a unified text-to-text transformer. *Journal of machine learning research*, 21(140):1–67, 2020. 3
- [36] Tanik Saikh, Tirthankar Ghosal, Amish Mittal, Asif Ekbal, and Pushpak Bhattacharyya. Scienceqa: A novel resource for question answering on scholarly articles. *International Journal on Digital Libraries*, 23(3):289–301, 2022. 1, 3
- [37] Dianmo Sheng, Dongdong Chen, Zhentao Tan, Qiankun Liu, Qi Chu, Jianmin Bao, Tao Gong, Bin Liu, Shengwei Xu, and Nenghai Yu. Towards more unified in-context visual understanding. In *Proceedings of the IEEE/CVF Conference on Computer Vision and Pattern Recognition*, pages 13362–13372, 2024. 5
- [38] Yi Tay, Mostafa Dehghani, Vinh Q. Tran, Xavier Garcia, Jason Wei, Xuezhi Wang, Hyung Won Chung, Dara Bahri, Tal Schuster, Huaixiu Steven Zheng, Denny Zhou, Neil Houlsby, and Donald Metzler. UL2: unifying language learning paradigms. In *Proceedings of International Conference on Learning Representations*, 2023. 3
- [39] Hugo Touvron, Thibaut Lavril, Gautier Izacard, Xavier Martinet, Marie-Anne Lachaux, Timothée Lacroix, Baptiste Rozière, Naman Goyal, Eric Hambro, Faisal Azhar, et al. Llama: Open and efficient foundation language models. *arXiv preprint arXiv:2302.13971*, 2023. 3
- [40] Lei Wang, Yi Hu, Jiabang He, Xing Xu, Ning Liu, Hui Liu, and Heng Tao Shen. T-sciq: Teaching multimodal chain-of-thought reasoning via large language model signals for science question answering. In *Proceedings of the AAAI Conference on Artificial Intelligence*, pages 19162–19170, 2024. 3
- [41] Xuezhi Wang, Jason Wei, Dale Schuurmans, Quoc V. Le, Ed H. Chi, Sharan Narang, Aakanksha Chowdhery, and Denny Zhou. Self-consistency improves chain of thought reasoning in language models. In *Proceedings of International Conference on Learning Representations*, 2023. 3
- [42] Yuqi Wang, Jiawei He, Lue Fan, Hongxin Li, Yuntao Chen, and Zhaoxiang Zhang. Driving into the future: Multiview visual forecasting and planning with world model for autonomous driving. In *Proceedings of the IEEE/CVF Conference on Computer Vision and Pattern Recognition*, pages 14749–14759, 2024. 1
- [43] Jason Wei, Maarten Bosma, Vincent Y. Zhao, Kelvin Guu, Adams Wei Yu, Brian Lester, Nan Du, Andrew M. Dai, and Quoc V. Le. Finetuned language models are zero-shot learners. In *Proceedings of International Conference on Learning Representations*, 2022. 3
- [44] Jason Wei, Xuezhi Wang, Dale Schuurmans, Maarten Bosma, Brian Ichter, Fei Xia, Ed H. Chi, Quoc V. Le, and Denny Zhou. Chain-of-thought prompting elicits reasoning in large language models. In *Proceedings of Annual Conference on Neural Information Processing Systems*, 2022. 2
- [45] Jason Wei, Xuezhi Wang, Dale Schuurmans, Maarten Bosma, Fei Xia, Ed Chi, Quoc V. Le, Denny Zhou, et al. Chain-of-thought prompting elicits reasoning in large language models. *Advances in Neural Information Processing Systems*, 35:24824–24837, 2022. 3
- [46] Junyi Yao, Yijiang Liu, Zhen Dong, Mingfei Guo, Helan Hu, Kurt Keutzer, Li Du, Daquan Zhou, and Shanghang Zhang. Promptcot: Align prompt distribution via adapted chain-of-thought. In *Proceedings of IEEE/CVF Conference on Computer Vision and Pattern Recognition*, pages 7027–7037, 2024. 2
- [47] Shunyu Yao, Dian Yu, Jeffrey Zhao, Izhak Shafran, Tom Griffiths, Yuan Cao, and Karthik Narasimhan. Tree of thoughts: Deliberate problem solving with large language models. *Advances in Neural Information Processing Systems*, 36, 2024. 3
- [48] Yao Yao, Zuchao Li, and Hai Zhao. Beyond chain-of-thought, effective graph-of-thought reasoning in language models. *arXiv preprint arXiv:2305.16582*, 2023. 3
- [49] Aohan Zeng, Xiao Liu, Zhengxiao Du, Zihan Wang, Hanyu Lai, Ming Ding, Zhuoyi Yang, Yifan Xu, Wendi Zheng, Xiao Xia, Weng Lam Tam, Zixuan Ma, Yufei Xue, Jidong Zhai, Wenguang Chen, Zhiyuan Liu, Peng Zhang, Yuxiao Dong, and Jie Tang. GLM-130B: an open bilingual pre-trained model. In *Proceedings of International Conference on Learning Representations*, 2023. 3
- [50] Jingyi Zhang, Jiaxing Huang, Sheng Jin, and Shijian Lu. Vision-language models for vision tasks: A survey. *IEEE Trans. Pattern Anal. Mach. Intell.*, 46(8):5625–5644, 2024. 1
- [51] Susan Zhang, Stephen Roller, Naman Goyal, Mikel Artetxe, Moya Chen, Shuohui Chen, Christopher Dewan, Mona Diab, Xian Li, Xi Victoria Lin, et al. Opt: Open pre-trained transformer language models. *arXiv preprint arXiv:2205.01068*, 2022. 3
- [52] Yuanhan Zhang, Kaiyang Zhou, and Ziwei Liu. What makes good examples for visual in-context learning? In *Proceed-*

- ings of Annual Conference on Neural Information Processing Systems*, 2023. 6
- [53] Zhuosheng Zhang, Aston Zhang, Mu Li, and Alex Smola. Automatic chain of thought prompting in large language models. In *Proceedings of International Conference on Learning Representations*, 2023. 3
- [54] Zhuosheng Zhang, Aston Zhang, Mu Li, Hai Zhao, George Karypis, and Alex Smola. Multimodal chain-of-thought reasoning in language models. *Trans. Mach. Learn. Res.*, 2024, 2024.
- [55] Ge Zheng, Bin Yang, Jiajin Tang, Hong-Yu Zhou, and Sibeil Yang. Ddcot: Duty-distinct chain-of-thought prompting for multimodal reasoning in language models. *Advances in Neural Information Processing Systems*, 36:5168–5191, 2023.
- [56] Denny Zhou, Nathanael Schärli, Le Hou, Jason Wei, Nathan Scales, Xuezhi Wang, Dale Schuurmans, Claire Cui, Olivier Bousquet, Quoc V. Le, and Ed H. Chi. Least-to-most prompting enables complex reasoning in large language models. In *Proceedings of International Conference on Learning Representations*, 2023. 3
- [57] Deyao Zhu, Jun Chen, Xiaoqian Shen, Xiang Li, and Mohamed Elhoseiny. Minigt-4: Enhancing vision-language understanding with advanced large language models. In *Proceedings of International Conference on Learning Representations*, 2024. 3
- [58] Deyao Zhu, Jun Chen, Xiaoqian Shen, Xiang Li, and Mohamed Elhoseiny. Minigt-4: Enhancing vision-language understanding with advanced large language models. In *Proceedings of International Conference on Learning Representations*, 2024. 3, 6, 7, 8, 9